



Aalborg Universitet

AALBORG UNIVERSITY
DENMARK

EOS Micro-Dose Protocol

First Full-spine Radiation Dose Measurements in Anthropomorphic Phantoms and Comparisons with EOS Standard-dose and Conventional Digital Radiology

Pedersen, Peter Heide; Petersen, Asger Greval; Østgaard, Svend Erik; Tvedebrink, Torben; Eiskjær, Søren P.

Published in:
Spine

DOI (link to publication from Publisher):
[10.1097/BRS.0000000000002696](https://doi.org/10.1097/BRS.0000000000002696)

Publication date:
2018

Document Version
Accepted author manuscript, peer reviewed version

[Link to publication from Aalborg University](#)

Citation for published version (APA):

Pedersen, P. H., Petersen, A. G., Østgaard, S. E., Tvedebrink, T., & Eiskjær, S. P. (2018). EOS Micro-Dose Protocol: First Full-spine Radiation Dose Measurements in Anthropomorphic Phantoms and Comparisons with EOS Standard-dose and Conventional Digital Radiology. *Spine*, 43(22), E1313–E1321. <https://doi.org/10.1097/BRS.0000000000002696>

General rights

Copyright and moral rights for the publications made accessible in the public portal are retained by the authors and/or other copyright owners and it is a condition of accessing publications that users recognise and abide by the legal requirements associated with these rights.

- Users may download and print one copy of any publication from the public portal for the purpose of private study or research.
- You may not further distribute the material or use it for any profit-making activity or commercial gain
- You may freely distribute the URL identifying the publication in the public portal -

Take down policy

If you believe that this document breaches copyright please contact us at vbn@aub.aau.dk providing details, and we will remove access to the work immediately and investigate your claim.

EOS® Micro-Dose Protocol: First Full-Spine Radiation Dose Measurements in Anthropomorphic Phantoms and Comparisons with EOS Standard-Dose and Conventional Digital Radiology (CR)

Peter Heide Pedersen, MD¹, Asger Greval Petersen, MSc, MPE², Svend Erik Østgaard, MD, PhD¹, Torben Tvedebrink, PhD³, Søren P. Eiskjær, MD¹

¹Department of Orthopedic Surgery, Aalborg Universitetshospital, Aalborg, Denmark

²Region Nordjylland, Røntgenfysik, Denmark

³Department of Mathematical Sciences, Aalborg University, Aalborg, Denmark.

Correspondence:

Peter Heide Pedersen
Ortopædkirurgisk Afdeling
Aalborg Universitetshospital
Hobrovej 18-22, 9000 Aalborg, Denmark
fax number: (+45)97662354, mobile phone: (+45)21129223, mail: php@rn.dk

The device(s)/drug(s) is/are FDA-approved or approved by corresponding national agency for this indication.

No funds were received in support of this work.

No relevant financial activities outside the submitted work.

Abstract

Study Design. A comparative study of radiation dose measured in anthropomorphic phantoms.

Objectives. First, to report the first organ dose and effective dose measurements in anthropomorphic phantoms using the new EOS imaging micro-dose protocol in full-spine examinations. Next, to compare these measurements of radiation dose to measurements in the EOS standard-dose protocol and CR.

Summary of Background Data. Few studies evaluating organ dose and effective dose for the EOS low-dose scanner exists, and mainly for the standard-dose protocol. To the best of our knowledge, no studies of effective dose based on anthropomorphic phantom measurements exists for the new micro-dose protocol.

Methods. Two anthropomorphic phantoms, representing a 5-year-old (pediatric) and a 15-year-old (adolescent). The phantoms were exposed to EOS micro-dose and standard-dose protocols during full-spine imaging. Additionally, CR in scoliosis settings was performed. For all modalities, organ doses were measured and effective doses were calculated using thermoluminescent dosimeters (TLD).

Results. We found a 17-fold reduction (94%) of effective dose in micro-dose protocol compared with our CR system in the adolescent phantom. Micro-dose versus standard-dose protocol, showed a 6-fold reduction (83%), and for standard-dose versus our CR system a 2.8-fold reduction (64%) reduction of effective dose was observed.

For the pediatric phantom, a 5-fold reduction (81%) of effective dose in micro-dose protocol compared to our CR system was observed. Micro-dose versus standard-dose protocol, showed a

7-fold (86%) reduction. However, we observed an increase in absorbed dose of 38% when comparing the EOS standard-dose protocol with our CR system.

Conclusions. The EOS imaging micro-dose option exposes patients to lower radiation doses than any currently available modality for full-spine examination. Expected reduction of dose was established for the adolescent phantom when comparing CR and standard-dose protocol.

However, no reduction of effective dose with EOS standard-dose protocol compared to our reference CR system was observed in the pediatric phantom.

Keywords: radiation dose, organ dose, effective dose, full-spine radiography, scoliosis, micro-dose, low-dose, anthropomorphic phantoms, cancer risk, cumulative dose, slot-scanning system, EOS stereo-radiography, phantom dosimetry.

Level of Evidence: N/A

Introduction

Adequate radiological imaging is required for the assessment and treatment of spinal deformity. Patients are frequently exposed to numerous radiographs; during diagnosis and treatment, whether conservative or surgical, and follow-up. The higher the total absorbed radiation dose, the higher is the risk of developing radiation-induced cancer. The atom bomb survivor studies¹ show a direct correlation between the total absorbed radiation dose and the risk of developing cancer. Especially children are at risk, since the stochastic damage caused by ionizing radiation often has a latency period of 1 or more decades before developing into cancer². A large cohort study³ showed a 68% increase in mortality, with a standard mortality ratio of 1.68 from breast cancer amongst a cohort of 5573 scoliosis patients followed for more than 40 years after being diagnosed and exposed to frequent radiographic examinations. Furthermore, a recent study indicated an increased risk of endometrial cancer amongst scoliosis patients as well⁴. To address this challenge, much effort has gone into optimizing radiologic equipment and finding alternatives to keep radiation dose as low as possible in order to decrease the risk of radiation-induced cancer while maintaining adequate image quality; commonly referred to as the ALARA principle (as low as reasonable achievable)⁵.

The EOS low-dose imaging system (EOS imaging®, Paris, France) has been developed to produce high quality images at low radiation doses⁶. We have been using the EOS scanner for full-spine examinations at our institution, since the fall of 2014. The EOS scanner uses a bi-planar slot-scanning technology, which has been described in detail elsewhere⁷⁻¹⁰. The original version of the system had a standard low-dose protocol. Lately, a micro-dose protocol with even lower dose imaging has become an option. EOS standard-dose setting has mainly been evaluated

with regards to skin entrance dose^{7,9,11}; however, only a few studies have evaluated organ dose and full-body absorbed dose (effective dose)¹⁰⁻¹².

The micro-dose protocol has so far mainly been evaluated in terms of image quality although an up to 45-fold reduction of absorbed radiation dose compared to CR has been stated¹³; a recent study reported effective dose estimates, based on the Monte Carlo dose-simulation program (PCXMC)¹⁴ using a mathematical phantom. The micro-dose protocol has previously been reported to provide the clinician with images comparable to CR^{13,15}.

The dual aim of our study was, first to report the first-ever organ dose and effective dose measurements in anthropomorphic phantoms using the EOS micro-dose protocol; second to compare our results to measurements in the EOS standard-dose protocol and CR.

Materials and methods

Phantom exposure

Two clinically validated anthropomorphic CIRS-ATOM® phantoms(-Computerized Imaging Reference System, Inc. Norfolk, VA., USA)¹⁶, a female adult (representing an adolescent) and a pediatric, were used. ATOM dosimetry phantoms have been designed to explore organ dose and effective dose, they consist of tissue equivalent epoxy resins and hold dosimeter locations specific to 21 inner organs.

Each phantom was positioned in the upright position within the EOS® scanner (Fig. 1). Full spine biplane radiological examinations were performed in two positions: anterior-posterior-lateral (APL) and posterior-anterior-lateral (PAL). Left lateral side of the phantom facing x-ray

source in the APL position and right lateral side in PAL. Vertical collimation with a laser positioning system was done in order to ascertain identical scan fields.

The micro-dose protocol shown in Table 1 differs from the standard-dose protocol by featuring increased cobber (Cu) filtration, decreased x-ray tube voltage (kV), and optimized image processing.

As previously described by *Damet et al*¹⁰, 20 consecutive scans were performed in each position in order to accumulate sufficient dose for measurements of the absorbed dose. The doses measured for each position were normalized into single examinations, and are listed as such in tables and figures. Measurements were done similarly for full-spine PA and AP, and subsequently, lateral (LAT) positions in CR (Siemens Ysio Max, Malvern, PA., USA), with CR long cassette wall stand, imaging parameters used are shown in Table 2. For CR LAT exposures, the right lateral side of the phantoms faced the x-ray-source according to in-house scoliosis protocol.

Dosimetry

TLD dosimeters (MCP-N, Krakow, Poland) were used for dosimetry. MCP-N dosimeters have a threshold of detecting radiation that is 200 times lower than more commonly used TLD-100 dosimeters.

Each TLD was placed within the phantoms at organ-specific positions and table-listed depths; eight dosimeters were placed on skin surfaces. All available internal dosimeter locations were used. The total of measuring points was in the range 184 (pediatric phantom) to 298(adolescent phantom). For calibration and dose readings, Rados IR-2000 irradiator and the Rados RE-2000

reader (RadPro International GmbH, Wermelskirchen, Germany) were used. Mean organ doses were measured, and effective doses were calculated as described in previous studies^{10,17}.

Effective dose (E), $E = \sum w_T H_T$, represents the full-body stochastic health risk, which is the probability of cancer induction and genetic effects, from any partial radiation of the body.

Effective dose is measured in millisieverts (mSv), and according to the International Commission on Radiological Protection (ICRP) publication 103⁵, calculated by summing the equivalent dose of each organ (H_T), which for x-ray radiation is equal to the average absorbed radiation dose for each organ, multiplied by a tissue-specific weighting (w_T) factor.

Statistical methods

Radiation dose was visualized by \log_{10} -transforming measurement data in order to compare standard-dose and micro-dose. Furthermore, this reduced variability of data observed due to the underlying proportionality in mean and variance. We used a negative binomial regression method in order to statistically model data. Data observation was used to identify the expected additive structure in mean for the radiation dose, i.e. the only interaction terms were between organs and the position of the phantom relative to the source (APL/PAL). From the statistical model, expected tissue/organ levels were estimated for the two directions (APL/PAL) with an additive term due to different dose protocols. Based on the estimated model parameters and associated standard errors, the ratio of absorbed dose was compared between CR, micro-dose and standard-dose. The estimated absorbed dose was evaluated using the estimated model parameters and tissue-factors from predetermined positions. The associated 95% confidence intervals were evaluated using parametric bootstrap similar to the mean estimate¹⁸. This parametric bootstrap was used in order to assess how the uncertainty in parameter estimates was

manifested in the absorbed dose. Main results have been expressed with 95% confidence intervals.

Results

Final inclusions

Adolescent phantom. All 290 internal TLD positions were available for TLD placement; so were 8 dosimeters placed on skin surfaces around the phantom. A few dosimeters were lost during dosimetry; 1-6 out of a total of 298 equal to 0.3-2% of the dosimeters used for calculating effective dose.

Pediatric phantom. A total of 176 out of 180 internal TLD positions were available for placement of dosimeters. Four positions lost were due to image quality insert cylinders. An additional 8 dosimeters were placed on the surface of the phantoms for skin dose measurements. In most positions and exposure-protocols a few dosimeters were lost during read-outs; either because they were broken or had fallen out. The number of lost dosimeters ranged from 0-2 per exposure-position, equal to 0-1% of the dosimeters used for calculating effective doses. Dosimeter readings from the three positions representing prostate and testes have not been included in the results; the phantoms represented females.

Effective doses

Figure 2 provides an overview of effective doses for both phantoms and exposure positions, including CR.

Adolescent phantom. We observed a 17-fold reduction (94%) of absorbed dose in micro-dose settings compared to measured dose absorbed with CR. Effective dose for PAL full spine, bi-

planar, radiographic examination with the micro-dose protocol was 29 μ Sv (27-31); the corresponding dose for CR PA-LAT was 491 μ Sv (456-531). A 6-fold reduction (83%) of effective dose was observed when comparing micro-dose with standard dose protocol. A 2.8-fold (64%) reduction of effective dose reduction was observed when comparing standard dose protocol with our CR system in PA-LAT.

Pediatric phantom. Effective dose for PAL full spine, bi-planar radiographic examination with the micro-dose protocol was 22 μ Sv (20-23); the corresponding dose for CR PA-LAT was 114 μ Sv (104-127); this is equivalent to a 5-fold reduction, (81%) of absorbed dose. A 7-fold reduction (86%) of effective dose was observed when comparing micro-dose with standard-dose protocol. However, there was an increase in absorbed dose of 38% when the EOS standard dose settings were compared with our CR system in PA-LAT.

Organ doses

Figures 3-6 demonstrate organ doses with micro-dose and standard-dose protocols for both phantoms, and show PAL/APL relations. For most organs, doses were lower in PAL than in APL. Effective doses in PAL compared with APL were reduced by an average of 21% (20-22%) for the phantoms in both standard and micro-dose protocols. The adolescent mean organ dose to the breasts was reduced by 29% in PAL; this reduction was solely on the left breast where dose was reduced from 403 μ Sv to 73 μ Sv, a 5.5-fold reduction, whereas the right breast dose was increased from 216 μ Sv to 287 μ Sv, a 33% increase in dose.

Discussion

To the best of our knowledge, the present study reports the first, anthropomorphic phantom based, measurements of effective dose and organ dose using the EOS micro-dose protocol. We

showed a significant reduction of absorbed doses using the micro-dose setting compared with a conventional system and to EOS standard-dose settings as summarized in Figure 2. We confirmed the manufacturer's claim that the micro-dose scan delivers radiation equal to less than 1 week of natural background radiation; viz. the mean weekly exposure is $46 \mu\text{Sv}$ ¹⁹. This finding corroborates that radiographic full-spine examinations can be performed without exposing the patient to more than very low amounts of ionizing radiation.

By presenting organ dose measurements in a micro-dose protocol and calculating the effective dose, we contribute to the ongoing evaluation of the risk of tissue detriment and death from radiation-induced cancer. With an average world-wide annual effective dose of 2.4 mSv (range 1-10) per capita¹⁹ from natural background exposure, a full-spine examination with micro-dose protocol and an effective dose of 22-37 μSv represents a very low dose. Two annual full-spine examinations with micro-dose protocol for 25 consecutive years would yield an accumulated effective dose below 2mSv, which is equivalent to less than 1 year of natural background exposure. Hence, the EOS micro-dose option offers full-spine imaging at an almost negligible radiation level. A recent study¹³ reports a 45-fold dose reduction with the micro-dose protocol compared with CR. This is, in fact, true if one was to compare to the dose delivered in conventional scoliosis full-spine examinations where radiation doses have been reported to reach around 3.5 mSv^{13,20}. As shown by our study, the CR dose with modern equipment used for AP-LAT spine imaging reached 0.545 mSv in the adolescent phantom. *Damet et al*¹⁰ found a comparable figure of 0.450 mSv for full-spine AP-LAT full-spine. Compared with our CR reference for PA-LAT full-spine doses, the micro-dose protocol offers a 17-fold reduction, which is still a marked reduction, but not in the means of 45-fold reduction. The radiation doses from modern systems have been much reduced [3, 21], and it seems that some reference guidelines for

full-spine effective doses need to be updated or reconsidered as far as the description of the dose reduction afforded by new systems is concerned.

Interestingly, in the pediatric phantom, our standard dose protocol showed no dose reduction compared with our reference CR. The child CR measurements were repeated and yielded same results. However, the PA-LAT CR dose of 114 μSv (104-127), for the pediatric phantom was not far from the 150 μSv for 4-7 year-olds, reported by Gialousis et al ²¹. Some of the explanation for the low dose for the small-child CR is likely attributable to conventional imaging optimization. Furthermore, we used a reduced-dose scoliosis protocol with right lateral exposure. Radiation exposure of the less radiation-sensitive right lateral side, has been reported to reduce lateral effective dose by up to 28% for children ²².

For the adolescent phantom we observed an effective dose reduction with EOS standard dose compared with CR, which is consistent with previous reports ^{10,11}. Our EOS standard-dose results for both phantoms are consistent with most reports ¹⁰⁻¹². Table 3 shows previously reported doses compared with the doses of the present study. Hui et al ¹⁴ reported an effective dose of 2.6 μSv for AP micro-dose projection, much lower than doses reported by any other study. We were surprised by this very low measure and have redone the calculations based on reported values. We found an effective dose of 3.1 μSv if we included the inherent aluminum filter of the EOS scanner in dose calculations, DAP values were used. If instead calculating effective dose from reported entrance skin dose, the effective dose was 5.2 μSv . The calculated values are closer to previously reported values but still very low. The exact reason is not known.

Organ doses to most organs were lower in PAL than in APL. Previous studies have documented that obtaining radiographs in the PA position decreases the amount of absorbed dose in most radiosensitive organs, and thus the effective dose [12, 22]. By measuring organ dose in both APL and PAL we were able to illustrate the dose divergence in the two positions for the EOS. The mean dose reduction in PAL versus PAL was 21%. A 29% mean dose reduction to the breasts was observed in the adolescent phantom. This is consistent with findings of *Luo et al*¹¹, when including lateral dose. The reported 8-fold reduction did not include lateral dose¹¹. The EOS PAL position should be favored as a means of reducing the previously reported elevated risk of breast cancer.

Historically, different methods have been applied for assessing organ dose and effective dose in the EOS scanner. Initially skin-entrance dose was described in comparisons of TLD measurements on skin surfaces with EOS and CR, and to calculate effective dose with the PCXMC method²⁴. *Clavel et al*¹² used GATE organ volume simulation with PCXMC to compare with TLD dose measurements. *Damet et al*¹⁰ reported organ dose and effective dose for the EOS standard protocol, based on measurements in anthropomorphic phantoms. The anthropomorphic phantoms provided us with a model closely mimicking the *in vivo* situation in terms of the anatomical placement of organs and tissue-equivalent materials. The setting allowed us to calculate patient organ doses and effective doses after direct exposure to dosimeters.

A limitation of the method used, is the fact that measurements were based on 20 consecutive scans in each position and normalized to one scan, instead of making a number of individual scans and measurements. *Damet et al*¹⁰ used only a fraction of available dosimeter placements (<25%) within the phantoms. Using only some of the predetermined dosimeter locations allows for considerable variations of dose measurements. For instance, four out of 28 TLD locations

were used in the liver for the adolescent phantom allowing for more than 20.000 possible combinations!

We chose to strengthen our study, by using all internal dosimeter locations. This allowed us to evaluate more precisely the mean absorbed dose within each organ. Furthermore, to address the uncertainties inherent in any studies within this area, we performed negative binomial regression analysis as described above.

This model provided a more flexible framework for count data interpretation, than the Poisson regression, in the case of potential overdispersion, which was the case in this study.

Even with new low-dose imaging we still have to keep focusing on ALARA, keeping the radiation dose as low as possible. The mean annual absorbed dose of ionizing radiation from medical causes is on the rise. Currently the annual absorbed dose is estimated at 1.2 mSv²⁵. So far, no lower threshold for the amount of ionizing radiation causing tissue damage, and potentially radiation-induced cancer has been established¹. Still, we need to devote efforts to keeping the risk from radiation-induced cancer from full-spine examinations lower than previously reported levels^{3,26}; and we need to continuously work towards minimizing the total radiation dose to which we expose our patients.

Acknowledgements:

We acknowledge the valuable support of University College Nordjylland (Radiografskolen), Selma Lagerløfs Vej 2, 9220 Aalborg Ø, Denmark, providing access to TLD irradiator and dose reader along with technical support.

References

1. Ozasa K, Shimizu Y, Suyama A, et al. Studies of the Mortality of Atomic Bomb Survivors , Report 14 , 1950 – 2003 : An Overview of Cancer and Noncancer Diseases. *Radiat Res* 2012;243:229–43.
2. Pace N, Ricci L, Negrini S. A comparison approach to explain risks related to X-ray imaging for scoliosis, 2012 SOSORT award winner. *Scoliosis* 2013;8:11.
3. Doody MM, Ronckers CM, Land CE, et al. Cancer mortality among women frequently exposed to radiographic examinations for spinal disorders. *Radiat Res* 2010;174:83–90.
4. A. S, S.B. C, K.E. J, et al. Incidence of cancer and infertility, in patients treated for adolescent idiopathic scoliosis 25 years prior. *Eur Spine J* 2015;24:S740.
5. ICRP Publication 103 The 2007 Recommendations of the International Commission on Radiological Protection.
6. Melhem E, Assi A, El Rachkidi R, et al. EOS(®) biplanar X-ray imaging: concept, developments, benefits, and limitations. *J Child Orthop* 2016;10:1–14.
7. Deschênes S, Charron G, Beaudoin G, et al. Diagnostic imaging of spinal deformities: reducing patients radiation dose with a new slot-scanning X-ray imager. *Spine (Phila Pa 1976)* 2010;35:989–94.
8. Yvert M, Diallo A, Bessou P, et al. Radiography of scoliosis: Comparative dose levels and image quality between a dynamic flat-panel detector and a slot-scanning device (EOS system). *Diagn Interv Imaging*. Epub ahead of print 2015. DOI:

10.1016/j.diii.2015.06.018.

9. Kalifa G, Charpak Y, Maccia C, et al. Evaluation of a new low-dose digital X-ray device: First dosimetric and clinical results in children. *Pediatr Radiol* 1998;28:557–61.
10. Damet J, Fournier P, Monnin P, et al. Occupational and patient exposure as well as image quality for full spine examinations with the EOS imaging system Occupational and patient exposure as well as image quality for full spine examinations with the EOS imaging system. *Med Phys*;63901. Epub ahead of print 2014. DOI: 10.1118/1.4873333.
11. Luo TD, Stans AA, Schueler BA, et al. Cumulative radiation exposure with EOS imaging compared with standard spine radiographs. *Spine Deform* 2015;3:144–50.
12. Clavel AH, Thevenard-Berger P, Verdun FR, et al. Organ radiation exposure with EOS: GATE simulations versus TLD measurements. 2016;9783:978352.
13. Ilharreborde B, Ferrero E, Alison M, et al. EOS microdose protocol for the radiological follow-up of adolescent idiopathic scoliosis. *Eur Spine J* 2016;25:526–31.
14. Hui SCN, Pialasse J-P, Wong JYH, et al. Radiation dose of digital radiography (DR) versus micro-dose x-ray (EOS) on patients with adolescent idiopathic scoliosis: 2016 SOSORT- IRSSD “John Sevastic Award” Winner in Imaging Research. *Scoliosis Spinal Disord* 2016;11:46.
15. Newton PO, Khandwala Y, Bartley CE, et al. New EOS Imaging Protocol Allows a Substantial Reduction in Radiation Exposure for Scoliosis Patients. *Spine Deform* 2016;4:138–44.
16. Body W, Organ D, Therapeutic D. ATOM Dosimetry Phantoms Size and Age Related

Dose Calculations Features :

17. Fujii K, Akahane K, Miyazaki O, et al. Evaluation of organ doses in CT examinations with an infant anthropomorphic phantom. *Radiat Prot Dosimetry* 2011;147:151–5.
18. Haukoos JS, Lewis RJ. Advanced statistics: Bootstrapping confidence intervals for statistics with “difficult” distributions. *Acad Emerg Med* 2005;12:360–5.
19. UNSCEAR. *SOURCES AND EFFECTS OF IONIZING RADIATION United Nations Scientific Committee on the Effects of Atomic Radiation*. 2010.
20. Mogaadi M, Ben Omrane L, Hammou A. Effective dose for scoliosispatients undergoing full spine radiography. *Radiat Prot Dosimetry* 2012;149:297–303.
21. Gialousis G, Yiakoumakis EN, Makri TK, et al. Comparison of dose from radiological examination for scoliosis in children among two pediatric hospitals by Monte Carlo simulation. *Heal Phys* 2008;94:471–8.
22. Ben-Shlomo A, Bartal G, Mosseri M, et al. Effective dose reduction in spine radiographic imaging by choosing the less radiation-sensitive side of the body. *Spine J* 2015;16:558–63.
23. Chaparian A, Kanani A, Baghbanian M. Reduction of radiation risks in patients undergoing some X-ray examinations by using optimal projections: A Monte Carlo program-based mathematical calculation. *J Med Phys* 2014;39:32–9.
24. Servomaa a., Tapiovaara M. Organ Dose Calculation in Medical X Ray Examinations by the Program PCXMC. *Radiat Prot Dosimetry* 1998;80:213–9.

25. Samara ET, Aroua A, Bochud FO, et al. Paper EXPOSURE OF THE SWISS POPULATION BY MEDICAL X-RAYS : 2008 REVIEW. 2012;263–70.
26. Doody MM, Lonstein JE, Stovall M, et al. Breast cancer mortality after diagnostic radiography: findings from the U.S. Scoliosis Cohort Study. *Spine (Phila Pa 1976)* 2000;25:2052–63.

ACCEPTED

Figure Legends:

Figure 1. A), Female phantom (representing an adolescent) in the EOS stereo-radiography scanner. Anterior-posterior-lateral (APL) position (frontal and lateral images are acquired simultaneously). **B),** Child phantom (representing a 5-year-old) in EOS scanner in APL position. **C,D),** Child phantom in the CR system in AP and LAT position (frontal and lateral images are acquired independently).



Figure 2. Effective doses for anthropomorphic phantoms with different imaging protocols. PAL (posterior-anterior + lateral exposure). APL (anterior-posterior + lateral exposure). CR (conventional digital radiology, scoliosis protocol), EOS st (EOS standard-dose protocol), EOS micro (EOS micro-dose protocol). Error bars represent 95% confidence intervals.

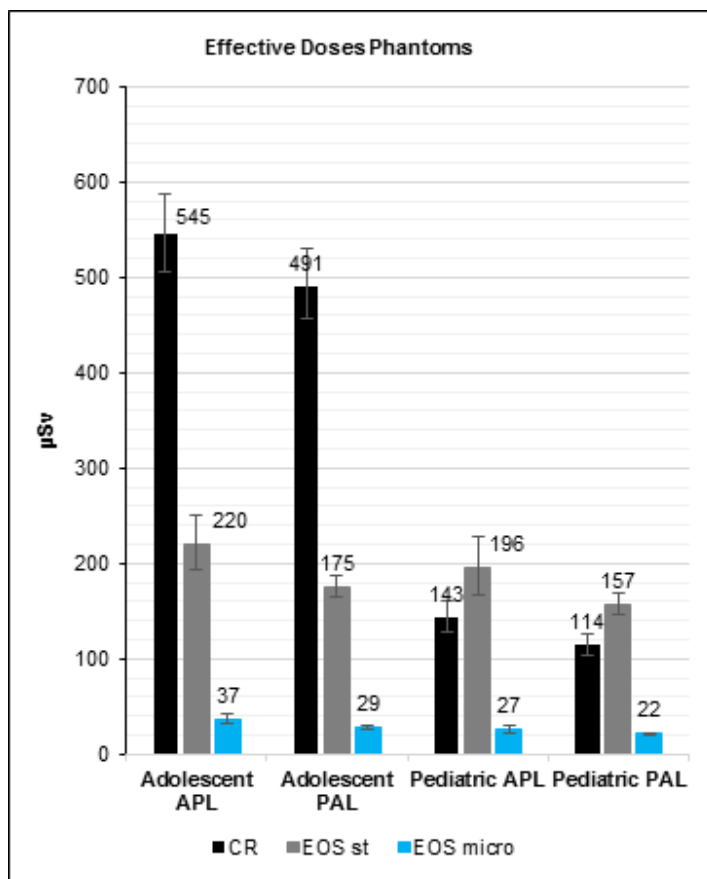


Figure 3. Mean organ doses in APL and PAL with micro-dose protocol, for the adolescent phantom. Error bars represent 95% confidence intervals.

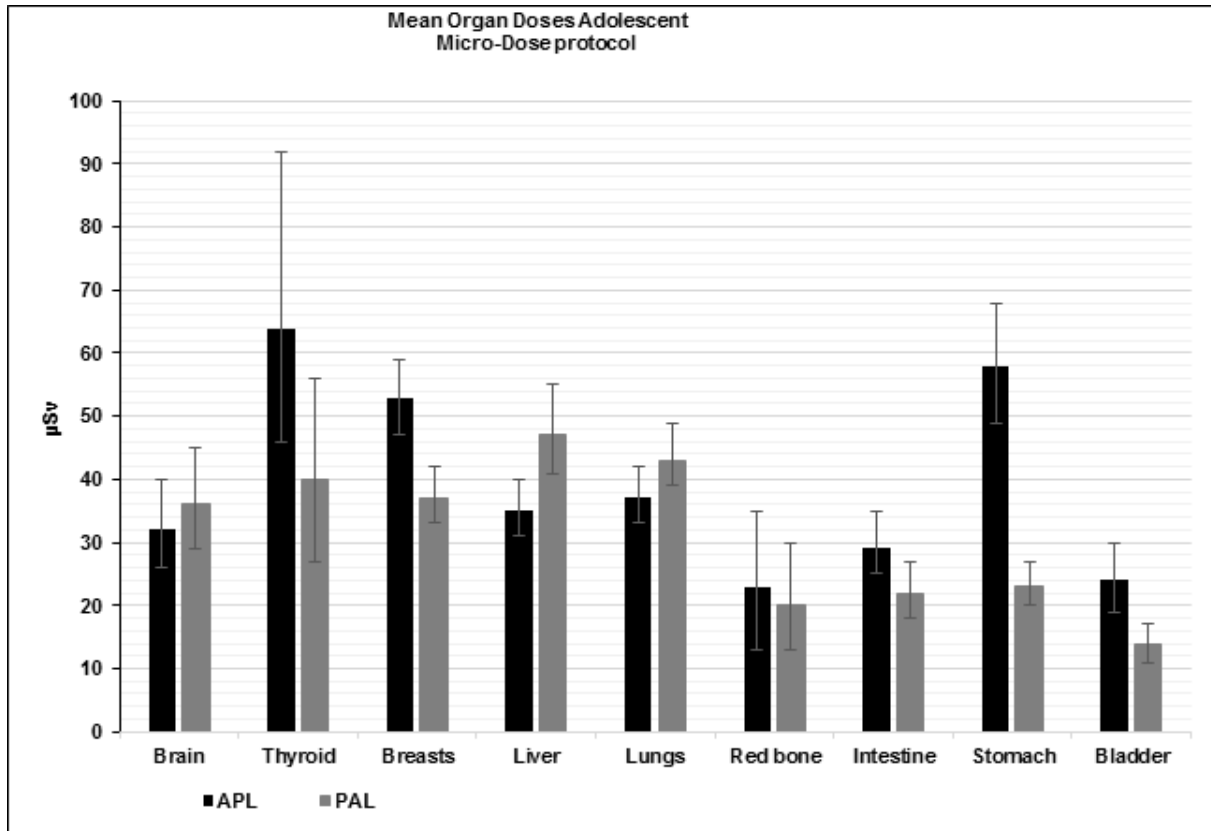


Figure 4. Mean organ doses in APL and PAL with standard-dose protocol, for the adolescent phantom. Error bars represent 95% confidence intervals.

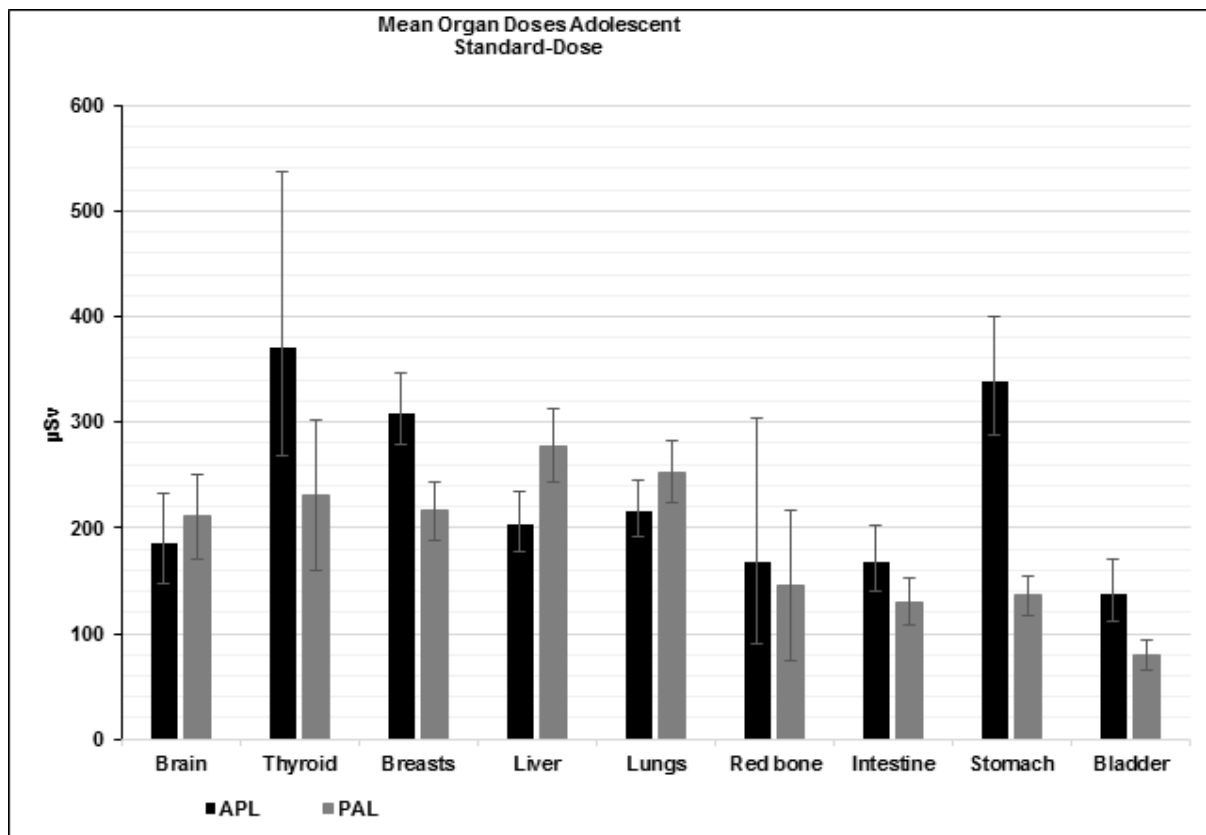


Figure 5. Mean organ doses in APL and PAL with micro-dose protocol, for the child phantom. Error bars represent 95% confidence intervals.

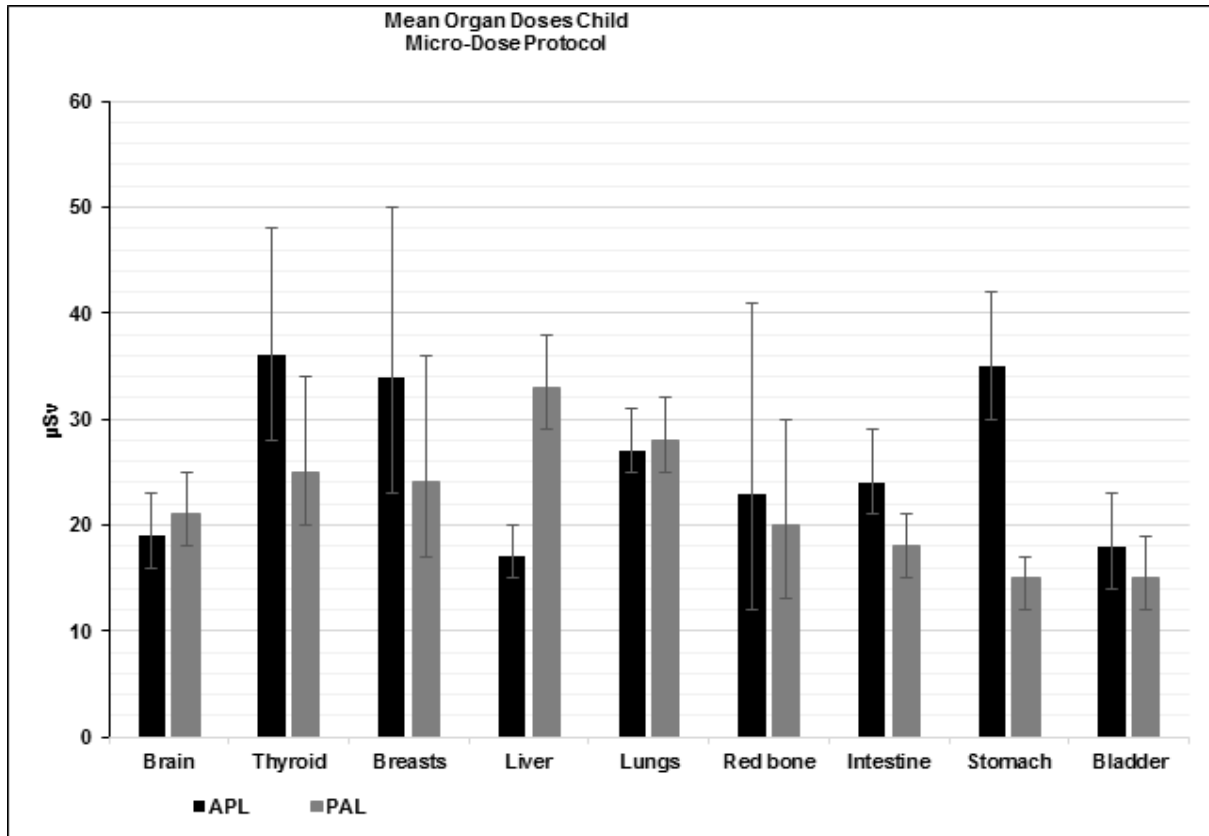


Figure 6. Mean organ doses in APL and PAL with standard-dose protocol, for the child phantom. Error bars represent 95% confidence intervals.

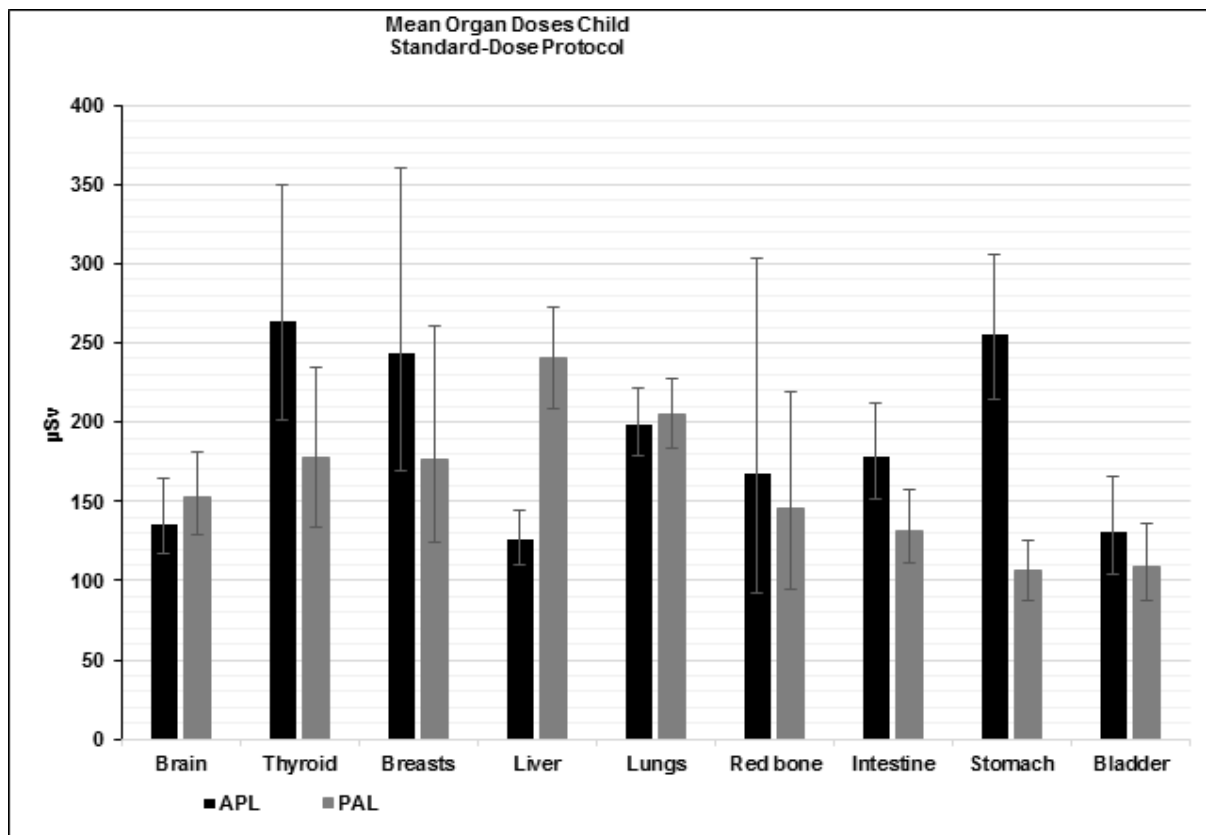


TABLE 1.EOS Scan Parameters				
	Female Pediatric Phantom	Female Pediatric Phantom	Female Adolescent phantom	Female Adolescent phantom
Protocols	Standard-Dose	Micro-Dose	Standard-Dose	Micro-dose
Morphotype	Small	Small	Medium	Medium
Scan Speed	4	3	4	4
Anterior X-Ray Tube				
kV	83	60	90	65
mA	200	80	250	80
DAP¹ (mG.cm²)	200	27	437	65
Lateral X-Ray Tube				
kV	102	80	105	90
mA	200	80	250	80
DAP(mG.cm²)	340	60	648	151

¹DAP = Dose area product

TABLE 2. CR Scoliosis Parameters (Siemens Ysio Max)		
CR scoliosis protocols¹	Pediatric Phantom	Female adolescent phantom
Anterior exposure		
kV	85	96
mAs	10	40
DAP(mGycm²)	120	1510
Lateral exposure²		
kV	90	102
mAs	16	63
DAP(mGycm²)	190	1470
¹ <i>Standard scoliosis protocols for 2-10 year-olds and for adults, used at our institution</i>		
² <i>Right lateral</i>		

TABLE 3. Previous Studies on Radiation Dose in EOS APL Standard-Dose Protocol

	Breasts, Mean, mSv	Thyroid, Mean, mSv	Ovaries Mean, mSv	Effective dose, mSv
Damet et al 2014 ¹⁰ (Adult Phantom)*	0.45	0.30	0.13	0.290
Luo et al 2015 ¹¹ (PCXMC, adult)	0.33	0.35	0.17	0.240
Present study (Adult Phantom)*	0.31	0.37	0.09	0.220

*Female adult phantom representing an adolescent